High precision monitoring of outgassing species in model extreme ultraviolet photoresists with a cavity ring-down spectrometer

Bernhard Lüttgenau,[a,*] Caleb Arata,[b] Honggu Im,[a] Maximillian Mueller,[a] Dahyun Oh,[c] Oleg Kostko,[a] Laura McHale,[b] Chris Rella,[b] John Hoffnagle,[b] Frances A. Houle[a]

[a] Lawrence Berkeley National Laboratory, Berkeley, California, United States

[b] Picarro, Inc., Santa Clara, California, United States

[c] San Jose State University, San Jose, California, United States

Abstract.

- **Background:** Extreme ultraviolet (EUV) photoresists play a pivotal role in advancing nanopatterning technologies by balancing image quality and sensitivity. The outgassing behavior of photoresist thin films under EUV and deep ultraviolet (DUV) exposure reveals chemical details relevant to their performance.
- **Aim:** This study focuses on utilizing an analytical technique not previously used in photolithography, the tabletop cavity ring-down spectrometer, to investigate outgassing dynamics in EUV photoresists, enabling precise chemical identification and deeper insights into resist processing.
- **Approach:** The spectrometer's enhanced laser path length (~20 km) and broadband absorption capabilities in the C-H overtone region allow for sensitive and temporally resolved detection of mixtures of outgassed species. Using a model resist comprising a polymer matrix with a photoacid generator and quencher, we analyzed the influence of time delays between exposure and post-exposure bake (PEB) as well as storage under varying environmental conditions.
- **Results:** Suppression of isobutylene outgassing and thickness loss was observed with extended delays between exposure and PEB, potentially linked to water absorption and acid deactivation. The technique proved highly effective in distinguishing subtle chemical differences between processing stages.
- **Conclusions:** Delay times and their environmental conditions, particularly humidity, reduce outgassing and thickness loss of photoresists during PEB, suggesting decreased acid-driven deprotection. This can potentially impact sensitivity, defectivity, and roughness of resist patterns, necessitating precise monitoring and control.

Keywords: Extreme ultraviolet photoresists, outgassing, cavity ring down spectroscopy, resist characterization, Extreme ultraviolet-induced chemistry.

* Bernhard Lüttgenau**,** E-mail: bluttgenau@lbl.gov

1 Introduction

The continued scaling of semiconductor devices relies on the development of advanced patterning technologies, where extreme ultraviolet (EUV) lithography has emerged as a key enabler for high-resolution manufacturing. A critical aspect of this process lies in the chemical performance of EUV photoresists, which must meet stringent requirements for sensitivity and resolution. The intricate interplay of radiation-induced chemical reactions during exposure and thermal chemistry during subsequent post-exposure bake (PEB) governs the efficacy of how the solubility of these materials in developer changes, making their precise characterization essential [1-4].

Among the many challenges in optimizing EUV photoresists is understanding how environmental conditions and processing delays influence chemical transformations within the resist film. Time delays between coating, exposure, and PEB, as well as storage conditions, can significantly affect these processes. For example, water absorption during extended delays may deactivate acids within the resist, affecting key reactions and performance outcomes [5].

Traditionally, mass spectrometry, reflectometry, and gas chromatography have been employed to analyze outgassing behavior in deep UV (DUV) [6-8] and EUV [9,10] chemically amplified resists. However, these methods can lack the ability to analyze mixtures with high sensitivity in real time, required for detailed studies of chemical reactions in thin polymer films. In this study, we introduce a tabletop cavity ring-down spectrometer as a novel analytical tool for identifying outgassed species with unprecedented sensitivity and temporal stability. Using a model resist comprising a polymer matrix with a photoacid generator and quencher, we investigate the role of different exposure types (EUV and DUV) and process delays on the chemical transformations within the resist. Our findings highlight the suppression of deprotection product outgassing after long delay times and explore the underlying mechanisms, offering pathways for enhanced resist design and processing.

2 Choice of Materials

In this work, we systematically investigate the properties of potential EUV resist materials, using a model resist consisting of the fundamental components of a chemically amplified photoresist (CAR), such as polymers, photoacid generators (PAG) and quenchers. This approach will allow for a clearer understanding of the capabilities and function of the novel characterization tool. The

polymer chosen for this study is a 6:4 random copolymer of *tert*-butylmethacrylate and 4-hydroxystyrene, referred to as P(tBMA-co-HS). Its detailed chemical structures are depicted in Figure 1. Triphenylsulfonium nonaflate was employed as the PAG, while triphenylsulfonium benzoate served as a photo decomposable quencher (PDQ). For the experiments presented here, the model resist formulation consisted of the pure polymer dissolved at 5.5 mg/mL in a 1:1 mixture of propylene glycol monomethyl ether (PGME) and propylene glycol methyl ether acetate (PGMEA). To this solution, 20 wt% PAG (relative to the polymer) and 100 mol% PDQ (relative to the PAG) were added. The polymer, PAG, and PDQ were synthesized by GreenCentre Canada. PGME and PGMEA were purchased from Sigma Aldrich. The resist was spin-coated on clean 100 mm Si wafers to achieve a homogeneous film thickness of ~17 nm. After spin-coating the samples underwent a post-application bake at 110 C for 60 s.

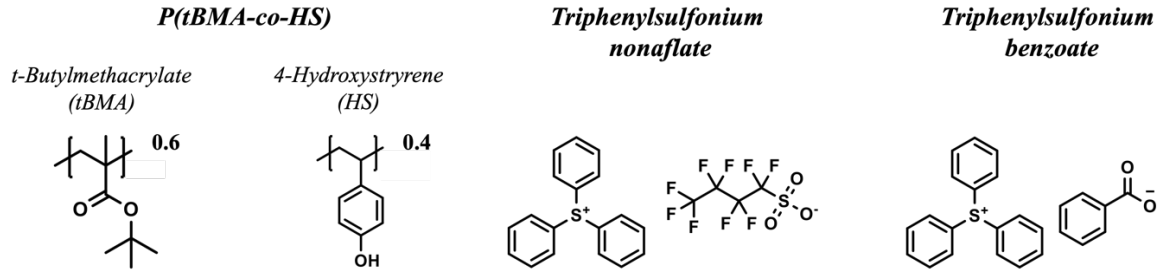

Fig. 1. Chemical structures of the investigated polymer, PAG and PDQ used to create model resist for evaluation of the characterization technique.

3 Experimental setup and technique

EUV exposures are conducted at beamline 12.0.1.2 of the Advanced Light Source (ALS), which provides tunable wavelengths in the EUV and soft X-ray range. For this study, the exposure wavelength is set to 13.5 nm, corresponding to the industry-standard EUV lithography wavelength. The setup accommodates 100 mm wafers and enables blanket EUV exposure with a spot size of 5 mm x 1 mm, ensuring uniform irradiation across the selected area. Different EUV doses are achieved by scanning the wafer in front of the EUV spot with velocities ranging from 0.01 mm/s to 1.35 mm/s. The light source intensity is tuned between 5 and 40 mJ/cm^2*s depending on the required dose. DUV exposures are performed using an Energetiq laser-driven light source (LDLS), where the broadband emission is filtered to isolate the 193 nm wavelength. This setup is capable of exposing wafers up to 200 mm in diameter, with a homogeneous quadratic exposure spot size of 1 cm x 1 cm. Different DUV doses are ensured by varying the exposure time. The light source

intensity is 0.16 mJ/cm^2*s. The controlled broadband filtering ensures a well-defined irradiation condition comparable to industrial DUV lithography processes.

In this study we focus on outgassing during PEB using a cavity ring-down spectrometer (CRDS) from Picarro, Inc. CRDS is a highly sensitive and precise technique for detecting molecular absorption, due to the long effective optical path of a laser beam that is resonant with a high-finesse optical cavity [11,12]. When the laser source is abruptly turned off, the intra-cavity optical field decays exponentially with a time constant that is a sensitive, quantitative measure of the cavity loss (see Fig. 2a). Keeping the cavity length fixed and using the periodic cavity resonances as an "optical frequency yardstick" provides a stable, accurate frequency axis for the absorption measurements (see Fig. 2b) [13]. The spectrometer used for this work incorporates a broadly tunable, frequency-agile laser source that emits light between about 1625 nm and 1710 nm, covering most of the first overtone of the C-H stretching vibration. Prior to undertaking the experiments for real-time sample analysis, least-squares fitting of the frequency-dependent absorption in the vibrational band permits differentiation between absorbing species, even with the same chemical formula, as well as simultaneous quantification of multiple species. This makes the spectrometer particularly well-suited for detecting outgassing compounds at extremely low concentrations, providing critical insights into the chemical processes occurring during PEB.

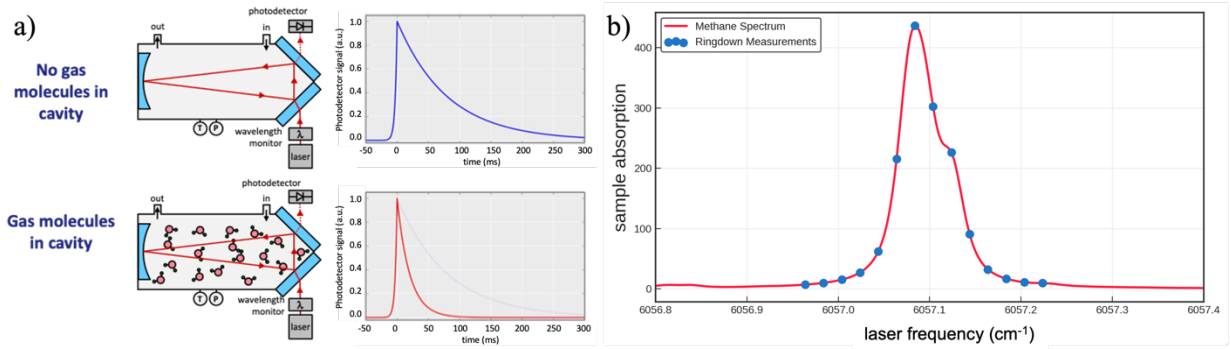

Fig. 2. Working principle of the cavity ring-down spectrometer (a) and exemplary measurement spectrum for methane (b).

To ensure efficient capture of all outgassing products, a sampling adaptor is affixed to the wafer, enclosing the resist surface and guiding the emitted species toward the CRDS detection system during the PEB. A controlled gas flow of 40 sccm is maintained within the setup to facilitate consistent sample transport and measurement conditions. The PEB process is simulated by placing the wafer on a programmable hotplate. First, the baseline (is linearly increased to 110 °C over 10

minutes and then held at 110 °C for 20 minutes. Finally, the hotplate is turned off to initiate the cool-down phase.

4 Results and discussion

In an initial study, we examined the generation of isobutylene, which we observe to be the primary acidolysis deprotection product formed during the PEB of the model resist after EUV exposure, consistent with prior work [14-16]. The sample was irradiated with an EUV dose of 30 mJ/cm² over an area of 15 cm². Figure 3 compares the detected isobutylene outgassing for both unexposed and exposed films during the PEB. The red trace shows the temperature profile, while the black trace plots the isobutylene signal in parts per billion (ppb). No isobutylene signal is observed for the unexposed sample, whereas a strong outgassing signal is recorded for the exposed sample. The data clearly demonstrate that the detection tool is highly sensitive to isobutylene released from the exposed regions of the film. Notably, the outgassing signal increases rapidly once the temperature exceeds 40 °C and reaches a maximum near 80 °C. After this point, the signal briefly decreases, then rises sharply again upon reaching 110 °C. Subsequently, the signal drops dramatically to below 10% of its maximum value. Once the hotplate is turned off, the signal promptly returns to zero.

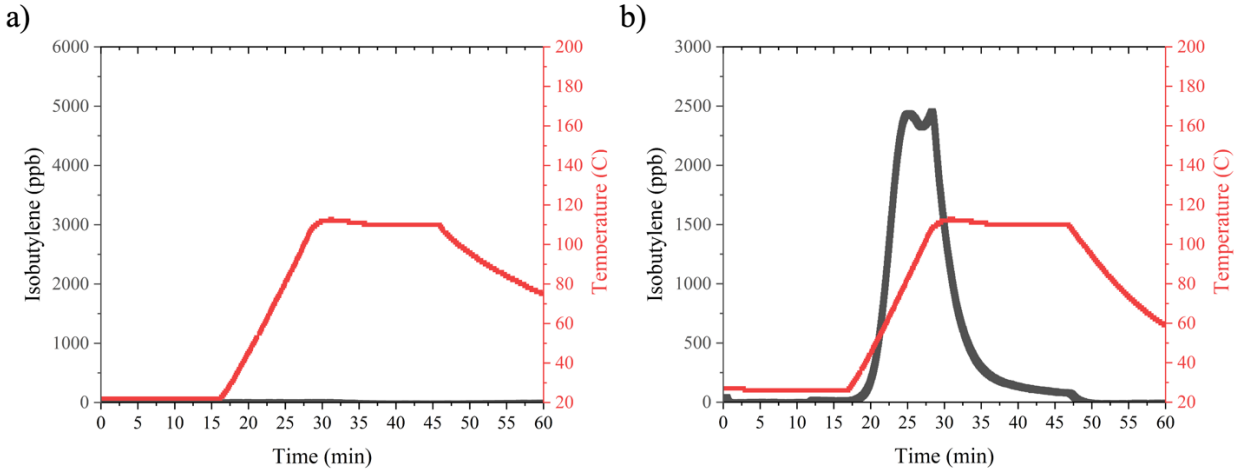

Fig. 3. Comparison of isobutylene signal during PEB as a function of time for two identical model resists with (b) and without (a) EUV exposure. The red curve shows the temperature profile during the PEB.

When comparing EUV-exposed model resists with different storage times between exposure and PEB, a pronounced influence of the storage time on the outgassing behavior is observed (see Fig. 4). After a 36-hour storage time, the outgassing from the EUV-exposed sample is

dramatically reduced, and it only commences at higher temperatures (>80 °C). This behavior suggests that two distinct mechanisms lead to deprotection of the tBMA monomers, resulting in isobutylene outgassing at low (<80 °C) and high (>80 °C) temperatures. As the storage time increases, the low-temperature outgassing fraction is not observed, whereas the second mechanism remains relatively unaffected. This could also account for the second high-temperature outgassing peak seen in the sample with a shorter (~3-hour) storage time between exposure and PEB.

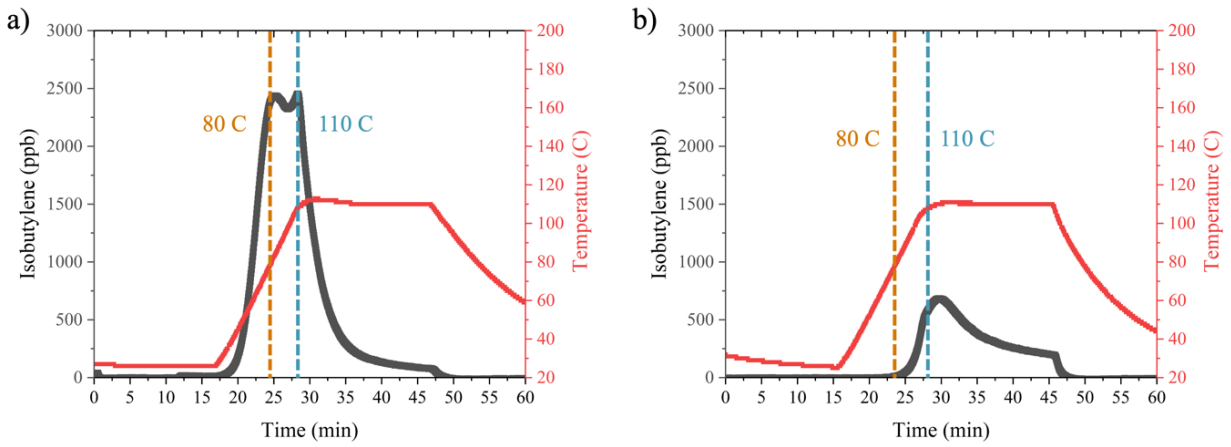

Fig 4. Comparison of isobutylene signal (black curve) during PEB as a function of time for two identical model resists with identical exposure conditions and storage times of 3h (a) and 36h (b) after exposure. The red curve shows the temperature profile during the PEB and dotted orange and blue vertical lines indicate the time at which 80 °C and 110 °C are reached.

To investigate this shift in outgassing behavior and its potential link to the deprotection mechanism of the polymer, we conducted a more comprehensive study of the storage time using DUV exposure at a wavelength of 193 nm. Using DUV exposure is an effective way to examine the process conditions and especially the activation of the PAG. Moreover, it offers better control over post-exposure delay times by circumventing the logistical constraints of synchrotron-based EUV sources.

To determine a suitable DUV exposure dose for the sample we compared outgassing signals for films exposed to varying DUV doses, ranging from 5 to 50 mJ/cm². Figure 5 presents both the contrast curve of the model resist for both a standard PEB of 60 s at 110 °C and the PEB used for the outgassing measurements (30 min with ~20 min at 110 °C) as well as the corresponding isobutylene outgassing signals measured during the longer PEB. The contrast curve exhibits a

strong dose response around 10 mJ/cm², with a dose-to-clear determined to be 12 mJ/cm². It can be seen, that the longer PEB exhibits the same dose-to-clear and can therefore be used as a good model for the PEB process. Additional dissolution tests also showed that the dose-to-clear does not change significantly with the storage time. A small thickness offset (< 2nm) can be noticed between wafers, especially for lower doses. This difference stems most likely from wafer-to-wafer spin speed variations and is within the ellipsometer uncertainty.

The outgassing signal is negligible for 5 mJ/cm², but increases markedly with dose thereafter. Even at 20 mJ/cm², the signal remains significantly higher than at 15 mJ/cm². For higher doses we see a plateau in the outgassing signal, followed by a decay of the signal for doses of 40 mJ/cm^2 and higher. The reason for this reduction in outgassing signal for higher doses is not clear, but could stem from extensive outgassing during the exposure [17,18]. Consequently, for all subsequent experiments, an exposure dose of 20 mJ/cm²—67% above the dose-to-clear—was chosen to ensure a stable outgassing signal.

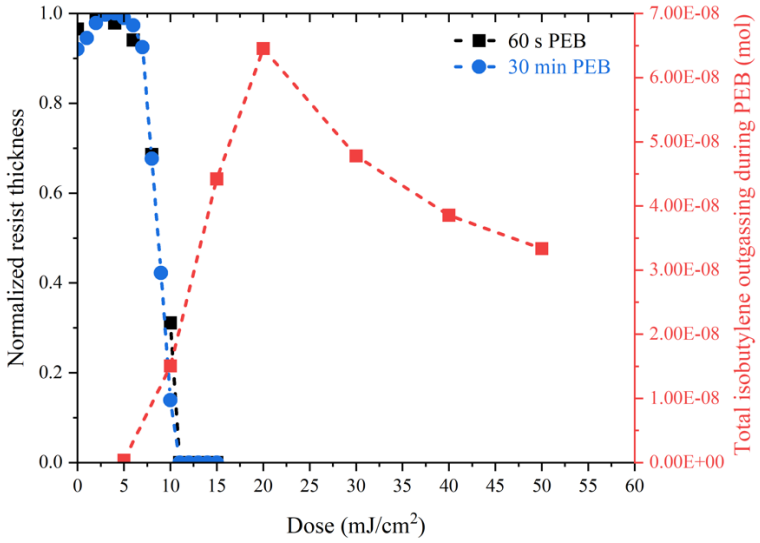

Fig. 5. Comparison of total isobutylene signal during PEB and the remaining film thickness after development for the EUV model resist as a function of DUV exposure dose for a regular 60 s PEB and the extended PEB (~30 min) used for the outgassing measurements.

Using the same model resist, we DUV-exposed samples to 20 mJ/cm² over an area of 15 cm². Figure 6 shows the resulting outgassing signals for samples processed immediately (Fig. 6a) and samples with a 24-hour storage under three storage conditions: nitrogen flow (Fig. 6b), ambient (Fig. 6c), and humid (Fig. 6d). Humid conditions were achieved by placing the exposed wafer in a sealed box containing an open water container to saturate the internal humidity. The results

clearly indicate that a 24-hour storage between exposure and PEB leads to a substantial reduction in the outgassing signal. Under ambient and humid conditions, the outgassing decreases by more than 90% compared to samples processed without storage. Even under continuous nitrogen flow, the signal is reduced by approximately 40%, although trace humidity is still present within the sample storage enclosure. Under ambient conditions the H_2O concentration is measured to ~1.14% with the CRDS tool, which corresponds to a relative humidity (RH) of ~50%. Under nitrogen flow, the H_2O concentration was measured to up to ~0.005%, which corresponds to ~0.22% RH. It remains unclear, if this trace level of humidity can result in the above seen reduction of the amount of outgassing.

Notably, the temperature at which the outgassing signal peaks also increases. In the absence of storage, the outgassing signal reaches a maximum at around 65 °C and diminishes close to zero by 110 °C. By contrast, the samples undergoing 24-hour storage time under ambient (~50% RH) and humid conditions (~100% RH) exhibit minimal outgassing until the temperature exceeds ~85 °C, with the peak outgassing occurring shortly after reaching 110 °C. It has to be noted that the double peak pattern visible in Fig. 4 becomes apparent only after extended storage times, as the contribution of the lower-temperature outgassing begins to significantly decrease. For short storage times (less than 5 minutes), the first peak dominates and obscures the second. Conversely, after very long storage times (~24 hours), the first peak is significantly diminished, and only the second peak remains clearly visible.

We may therefore conclude that exposure to humidity or other chemical components of the ambient air (e.g. NH_3 or oxygen) during storage leads to a deactivation of the generated acid within the film, which in turn inhibits or reduces the efficiency of deprotection during the PEB. The impact of NH_3 on DUV photoresists has been studied extensively [19]. Reported pathways - direct acid neutralization, base diffusion into the resist film, and substrate-derived bases - all remove catalytic protons and degrade resist performance. Typical indoor NH_3 levels are 10-70 ppb and can rise in occupied rooms [20]. In our experiments, NH_3 concentrations were only 4.3 ppb in ambient air and 3.4 ppb under a continuous N_2 purge, indicating that ammonia is not the primary cause of the observed acid loss.

Water uptake, on the other hand, is known to raise the dose-to-clear in systems such as t-BOC-protected poly(hydroxystyrene) (PHS) [5]. Moisture swells the resist film and introduces

additional proton-trap sites, reducing acid mobility and slowing deprotection. If additional quenchers are present in the resist film, this can lead to over-quenching and altered critical dimensions. The cavity-ring-down spectroscopy (CRDS) tool employed in this study now allows us to quantify directly how storage conditions affect the PEB chemistry and the associated deprotection mechanisms.

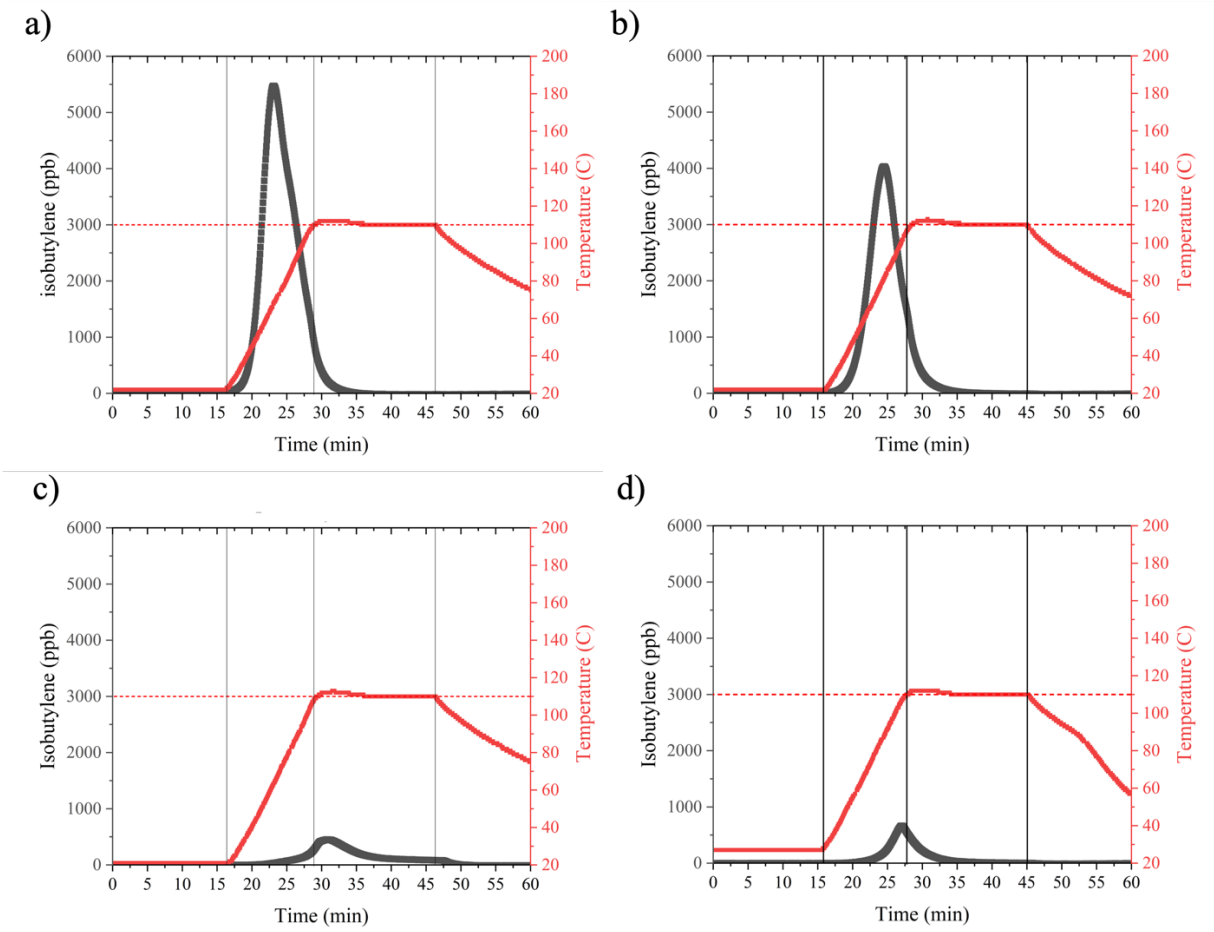

Fig. 6. Comparison of isobutylene signal (black curve) during PEB as a function of time for identical DUV-exposed model resists with identical exposure conditions with storage times of ~3min (a) and 24h under each condition (b) constant nitrogen flow, (c) ambient conditions and (d) increased humidity. The red curve shows the temperature profile used for the PEB. Red dotted horizontal line indicates 110 °C, black vertical lines indicate the start of PEB, final temperature and start of cool-down (left to right).

The CRDS tool also enables the quantification of the total outgassing volume by integrating over the outgassing signal in ppb and multiplying it with the total gas flow inside the tool (40 sccm). By assuming an ideal gas, one can then calculate the total number of outgassing isobutylene molecules in moles. Figure 7 provides an overview of the total isobutylene outgassing from an average film volume of 2.55×10^{-5} cm^3, measured during PEB for DUV-

exposed samples stored under various conditions. Storage times ranged from 3 minutes to 24 hours under ambient conditions, and additional 24-hour storage times were carried out under humid, vacuum, and nitrogen environments. Vacuum conditions were achieved by placing the wafer in a vacuum chamber at an average pressure of 5×10^{-7} Torr. The data reveal a progressive decline in outgassing with longer ambient storage times, with reductions of approximately 10% after one hour and as much as 85% after 24 hours. Storing samples under vacuum or nitrogen flow substantially reduced these effects, resulting in a 60% decrease in outgassing after 24 hours of vacuum storage and a 40% decrease under nitrogen. Notably, the vacuum-storage protocol includes a 20-minute transfer in a nitrogen-filled bag. Although the modest drop in outgassing within the first hour likely does not markedly affect the dose-to-clear of the samples, it could alter the deprotection behavior of the tBMA segments in P(tBMA-co-HS) within the film and potentially cause pattern defects. Additional in-depth studies will be necessary to fully understand these effects.

Comparing these values to the estimated number of tBMA segments in P(tBMA-co-HS) in the exposed film volume—calculated to be approximately 8.5×10^{-8} moles (for an area of 15 cm² and thickness of 17 nm)—shows that, in the absence of a storage delay, around 75% of the total isobutylene in the film is released during PEB.

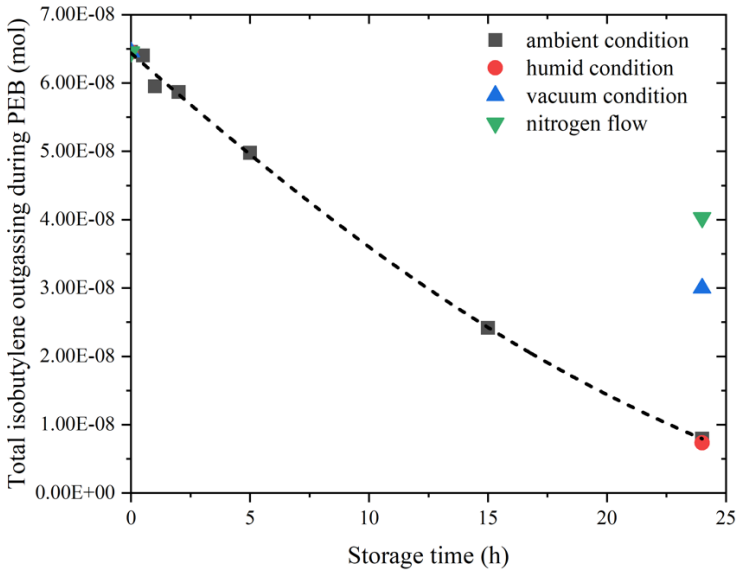

Fig. 7. Comparison of the absolute isobutylene outgassing during PEB in moles for different storage times between DUV-exposure and PEB under different storage conditions. The black dashed line is inserted to guide the eye.

To further elucidate the effect of storage conditions, we measured the film thickness of selected samples following coating, DUV exposure with 20 mJ/cm^2, and PEB (see Fig. 8). These samples were either processed with minimal storage time (less than three minutes) or stored for 24 hours under ambient, humid, or vacuum conditions. Immediately after the DUV exposure step the film thickness was consistently reduced by 2 nm. This could stem from the outgassing of sulfur-containing PAG components [6,7]. By contrast, the thickness changes attributable to PEB depended strongly on the storage conditions. For minimal storage times, the additional thickness loss during PEB was about 3.5 nm, nearly double the reduction observed during exposure. One has to note here, that due to the ellipsometer measurement after exposure, there was an unavoidable delay, that lead to a reduction in outgassing of ~20% compared to a sample without delay. Under vacuum storage conditions, the PEB-related thickness loss was around 3 nm, despite notably lower outgassing of isobutylene measured during PEB. That indicates additional outgassing of species (e.g. PAG-components) during the PEB, that have a significant influence on the film shrinkage [6,7].

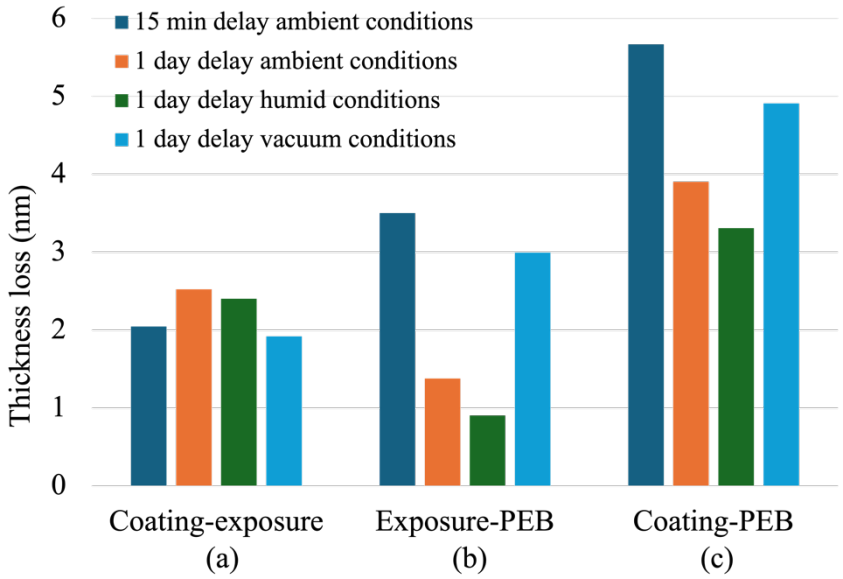

Fig. 8. Comparison of absolute thickness loss during different process steps for identical model resists with identical exposure conditions and different storage times and conditions between exposure and PEB. Absolute thickness loss was compared for samples after coating and immediately after exposure (a), immediately after exposure and immediately after PEB (b), and after coating and immediately after PEB (c).

Additionally, the shrinkage during the storage time under vacuum conditions is not measured, which could contribute to the overall film shrinkage. As a result, despite the significant difference in isobutylene outgassing levels during PEB, the overall thickness change remains comparable. Meanwhile, for samples stored for 24 hours under ambient and humid conditions,

the film thickness loss was approximately 1.3 nm and 0.9 nm, respectively. These results indicate that the observed reduction in outgassing during PEB is primarily due to partial deactivation of the deprotection mechanism, rather than to any prior outgassing during storage.

To investigate the shift of the peak outgassing signal from lower temperatures to higher temperatures during the PEB, we performed a study with a two-step PEB process and storage under ambient conditions. First the sample underwent a PEB process with the time profile shown Fig. 3a up to a maximum temperature of 80 °C. After cooling down to a temperature below 30 °C, the sample underwent a second PEB process up to 110 °C. The temperature profile is shown in Figure 9.

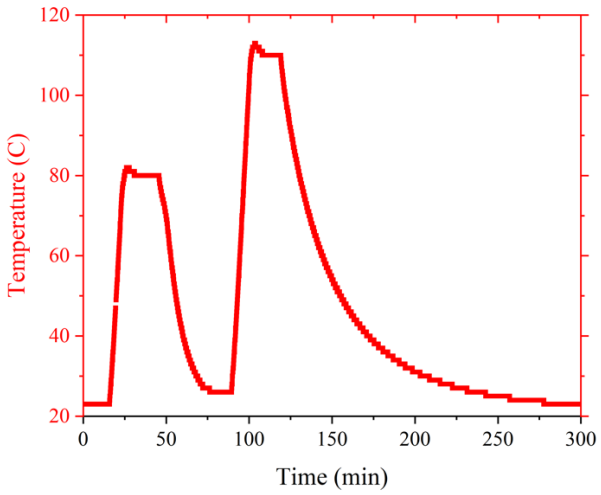

Fig. 9. Temperature profile for the separated PEB process with temperatures of 80 °C and 110 °C.

Figure 10 shows the comparison of total outgassing for both steps of the PEB process for the model resist. We again see a clear dependence of the individual outgassing signals on the storage time. While the outgassing during the first low-temperature PEB declines strongly, the outgassing signal at the second high-temperature PEB increases only modestly with storage time.

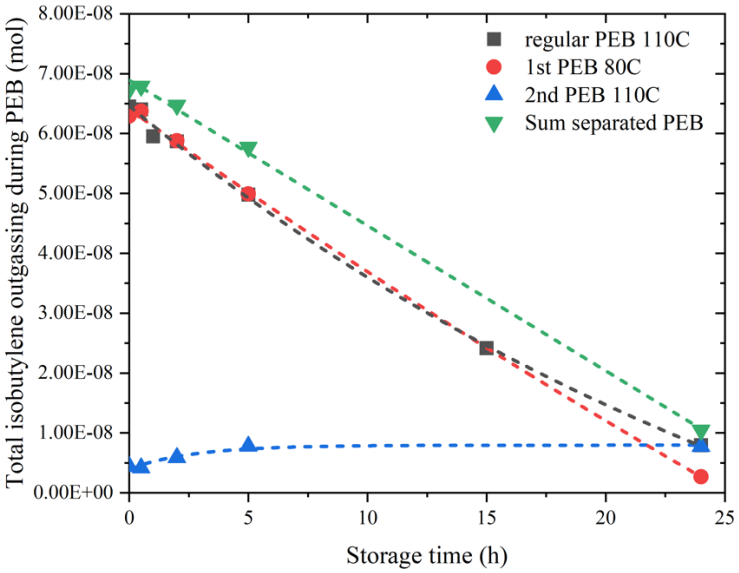

Fig. 10. Comparison of total isobutylene outgassing in moles for model resist and different delay times under ambient conditions. The black squares show the outgassing levels for a regular PEB up to 110 °C. The red circles show the outgassing for a PEB up to 80 °C and the blue triangles show the outgassing for a consecutive PEB up to 110 °C. The green inverted triangles show the sum of outgassing during both separated PEB processes. Dashed lines are inserted to guide the eye.

Additionally, the total outgassing during the 80 °C PEB process matches the outgassing from the regular PEB process up to 110 °C within the uncertainties of the measurement method. This indicates that, especially for shorter storage times below 5h, a PEB temperature of 80 °C is sufficient to create the same amount of isobutylene outgassing from the film. The observed outgassing during the second exposure step therefore does not indicate a different deprotection mechanism but additional outgassing due to additional thermal activation of the acid inside the film.

5 Conclusion and outlook

In summary, our investigation demonstrates that both humidity and storage conditions have a profound impact on acid activity within the film, the subsequent acid-catalyzed deprotection of tBMA segments in P(tBMA-co-HS), and overall outgassing behavior during the post-exposure bake. Using CRDS as a real-time detection tool, we established that delaying the PEB for several hours can significantly suppress isobutylene release, particularly under ambient and humid conditions. This suppression likely arises from acid deactivation by moisture and translates into reduced deprotection of the polymer during PEB, as confirmed by lower outgassing signals and

smaller final thickness losses. Dissolution measurements do not show a significant change in the dose-to-clear after extended storage times.

In contrast, storage in vacuum and nitrogen preserve a portion of the generated acid, reducing the extent of outgassing decay over time. Although these storage conditions still produce a measurable decrease in outgassing, the effect is less pronounced than under ambient or humid environments. Film thickness measurements reveal that storage in vacuum, despite lower outgassing, can still lead to substantial thickness changes.

Taken together, these results emphasize the need to carefully control environmental conditions and delay between exposure and PEB to ensure repeatable process performance. The ability to quantitatively detect and compare outgassing products under varying storage conditions provides critical insights into the deprotection mechanisms of EUV and DUV resists, ultimately guiding strategies for improved lithographic pattern fidelity and process stability.

While this study focused on a single chemically amplified resist (CAR) platform, the demonstrated sensitivity and accuracy of the CRDS technique make it broadly applicable to other CARs as well as molecular resists (MORs). Future investigations should explore these additional platforms to expand the scope and validate generalizability. Moreover, ongoing efforts to enable sampling under vacuum conditions may pave the way for real-time outgassing diagnostics across multiple process steps, providing deeper insight into material behavior during lithographic processing.

Data Availability

The data that support the findings of this study are available here:
https://osf.io/w5dyt/?view_only=f12a3fb04bf2443b907f1a90e49589b7

Disclosures

The authors declare there are no financial interests, commercial affiliations, or other potential conflicts of interest that have influenced the objectivity of this research or the writing of this paper.

Acknowledgments

This work was supported as part of the Center for High Precision Patterning Science (CHiPPS), an Energy Frontier Research Center funded by the U.S. Department of Energy, Office of Science,

Basic Energy Sciences at Lawrence Berkeley National Laboratory under Contract No. DE-AC02-342 05CH11231. This research used resources at the Advanced Light Source operated by Lawrence Berkeley National Laboratory under Contract No. DE-AC02-05CH11231, a U.S. Department of Energy (DOE) Office of Science User Facility.

References

1. Wang, X., Tao, P., Wang, Q., Zhao, R., Liu, T., Hu, Y., Hu, Z., Wang, Y., Wang, J., Tang, Y., Xu, H., He, X., "Trends in photoresist materials for extreme ultraviolet lithography: A review," Materials Today (67), (2023) 299-319

2. Kozawa, T., Tagawa, S., "Radiation Chemistry in Chemically Amplified Resists", Japanese Journal of Applied Physics 49, 030001 (2010).

3. Narasimhan, A., Wisehart, L., Grzeskowiak, S., Ocola, L. E., Denbeaux, G., Brainard, R. L., "What We Don't Know About EUV Exposure Mechanisms", Journal of Photopolymer Science and Technology, 30, Issue 1, Pages 113-120 (2017).

4. Hinsberg, W. D., Wallraff, G. M., Sanchez, M. I., Megiddo, N., and Kostko, O., "Contribution of EUV resist counting statistics to stochastic printing failures", J. Micro/Nanopattern. Mater. Metrol. 20(1), 014603-1 (2021).

5. Burns, S. D., Medeiros, D. R., Johnson, H. F., Wallraff, G. M., Hinsberg, W. D., Willson, C. G., "Effect of humidity on deprotection kinetics in chemically amplified resists", Proc. of SPIE, 4690, p. 321-331 (2002).

6. Houle, F. A., Deline, V. R., Truong, H., Sooriyakumaran, R., "Characterization of Volatile Species Formed during Exposure of Photoresists to Ultraviolet Light", Macromolecules 40 (21), 7505-7512 (2007).

7. Houle, F. A., Maxim, N., Huijbregtse, J., Deline, V. R., Truong, H., van Schaik, W., "Quantification of outgassing of C-, Si-, and S-containing products during exposure of photoresists," J. Vac. Sci. Technol. B 27 (2), 654–664 (2009).

8. Hinsberg, W. D., Houle, F. A., Poliskie, G. M., Pearson, D., Sanchez, M., Ito, H., "Product Volatilization as a Probe of the Physics and Chemistry of Latent Image Formation in Chemically Amplified Resists", J. Phys. Chem. A, 106, 9776-9787 (2002).

9. Grzeskowiak, S., Kaminsky, J., Gibbons, S., Narasimhan, A., Brainard, R. L., Denbeaux, G., "Electron trapping: a mechanism for acid production in extreme ultraviolet photoresists," J. Micro/Nanolith. MEMS MOEMS 17(3), 033501 (2018).

10. Tarrio, C., Benner, B. A., Vest, R. E., Grantham, S., Hill, S. B., Lucatorto, T. B., Hendricks, J. H., Abbott, P., Denbeaux, G., Mbanaso, C., Antohe, A., Orvek, K., Choi, K.-W., "Quantitative measurement of outgas products from EUV photoresists," Proc. SPIE 6921, Emerging Lithographic Technologies XII, 69211H (2018).

11. Anderson, D.A., Frisch, J.C., Masser, C.S., "Mirror reflectometer based on optical cavity decay time," Appl. Opt. 23, 1238 (1984).

12. Crosson, E.R., "A cavity ring-down analyzer for measuring atmospheric levels of methane, carbon dioxide, and water vapor," Appl. Phys. B 92, 403 (2008).

13. Steig, E. J., Gkinis, V., Schauer, A. J., Schoenemann, S. W., Samek, K., Hoffnagle, J., Dennis, K. J., and Tan, S. M., "Calibrated high-precision ^{17}O-excess measurements using cavity ring-down spectroscopy with laser-current-tuned cavity resonance," Atmos. Meas. Tech., 7, 2421–2435 (2014).

14. Fu, C., Du, K., Xue, J., Xin, H., Zhang, J. and Li, H., "Mechanisms of acid generation from ionic photoacid generators for extreme ultraviolet and electron beam lithography," Phys. Chem. Chem. Phys. (26), 18547-18556 (2024)

15. Mbanaso, C., Kruger, S., Higgins, C., Khopkar, Y., Antohe, A., Cardineau, B., Denbeaux, G., "Mass spectrometer characterization of reactions in photoresists exposed to extreme ultraviolet radiation", Proc. of SPIE 7969, 79692J (2011).

16. Luttgenau, B., Arata, C., Im, H., Mueller, M., Oh, D., Kostko, O., McHale, L., Rella, C., Hoffnagle, J., Houle, F. A., "High precision monitoring of outgassing species in model EUV photoresists with a cavity ring-down spectrometer", Proc. of SPIE 13428, 134281R (2025).

17. Luttgenau, B., Zhang, M., Zhang, Q., Wang, C., Ruiz, R., Connolly, M., Kostko, O., "Time-dependent characterization of total electron yield and outgassing in model EUV resist materials," Proc. of SPIE 13215, 132150H (2024).

18. Luttgenau, B., Im, H., Zhang, M., Zhang, Q., Wang, C., Ruiz, R., Connolly, M., Kostko, O., "Polypeptoids as promising EUV photoresists: a study of total electron yield and outgassing under EUV exposure," Proc. of SPIE 13428, 134281L (2025).

19. Kishkovich, O.P., Larson, C. E., "Amine control for DUV lithography: identifying hidden sources", Proc. of SPIE, 3999, Advances in Resist Technology and Processing XVII, (2000).

20. Li, M., Weschler, C. J., Bekö, G., Wargocki, P., Lucic, G., Williams, J., "Human Ammonia Emission Rates under Various Indoor Environmental Conditions", Environmental Science & Technology 54 (9), 5419-5428, (2020).

Caption List

Fig. 1 Chemical structures of the investigated polymers, PAG and PDQ used to create model resist for evaluation of the characterization technique.

Fig. 2 Working principle of the cavity ring-down spectrometer (a) and exemplary measurement spectrum for methane (b).

Fig. 3 Comparison of isobutylene signal during PEB as a function of time for two identical model resists with (b) and without (a) EUV exposure. The red curve shows the temperature profile during the PEB.

Fig. 4 Comparison of isobutylene signal (black curve) during PEB as a function of time for two identical model resists with identical exposure conditions and storage times of 3h (a) and 36h (b) after exposure. The red curve shows the temperature profile during the PEB and dotted orange and blue vertical lines indicate the time at which 80 °C and 110 °C are reached.

Fig 5 Comparison of total isobutylene signal during PEB and the remaining film thickness after development for the EUV model resist as a function of DUV exposure dose for a regular 60 s PEB and the extended PEB (~30 min) used for the outgassing measurements.

Fig. 6 Comparison of isobutylene signal (black curve) during PEB as a function of time for identical DUV-exposed model resists with identical exposure conditions with storage times of ~3min (a) and 24h under each condition (b) constant nitrogen flow, (c) ambient conditions and (d) increased humidity. The red curve shows the temperature profile used for the PEB. Red dotted horizontal line indicates 110 °C, black vertical lines indicate the start of PEB, final temperature and start of cool-down (left to right).

Fig. 7 Comparison of the absolute isobutylene outgassing during PEB in moles for different storage times between DUV-exposure and PEB under different storage conditions. The black dashed line is inserted to guide the eye.

Fig. 8 Comparison of absolute thickness loss during different process steps for identical model resists with identical exposure conditions and different storage times and conditions between exposure and PEB. Absolute thickness loss was compared for samples after coating and immediately after exposure (a), immediately after exposure and immediately after PEB (b), and after coating and immediately after PEB (c).

Fig. 9 Temperature profile for the separated PEB process with temperatures of 80 °C and 110 °C.

Fig. 10 Comparison of total isobutylene outgassing in moles for model resist and different delay times under ambient conditions. The black squares show the outgassing levels for a regular PEB up to 110 °C. The red circles show the outgassing for a PEB up to 80 °C and the blue triangles show the outgassing for a consecutive PEB up to 110 °C. The green inverted triangles show the sum of outgassing during both separated PEB processes. Dashed lines are inserted to guide the eye.

Biographies

Bernhard Lüttgenau received his doctoral degree in 2024 from RWTH Aachen University, Germany, where he conducted research on EUV interference lithography employing partially coherent EUV sources. His current research as a Research Scientist at Lawrence Berkeley National Laboratory focuses on the fabrication and design of advanced nano-diffractive optics. He also investigates EUV resist materials using advanced spectroscopic techniques with EUV and soft X-ray radiation.

Dahyun Oh received her BS and PhD in materials science and engineering from Seoul National University and the Massachusetts Institute of Technology (MIT), respectively. After completing her PhD, she continued her biomaterials project at MIT as a postdoctoral associate in 2014. In 2015, she joined the IBM Almaden Research Center as a research scientist, where she studied in situ gas analysis techniques for energy storage devices. Since joining San Jose State University in 2017 as an assistant professor, her research group has focused on studying liquid and solid interfacial reactions for various applications, including electrochemical devices, photoresists, and antifungal films.

Oleg Kostko obtained his doctoral degree from the University of Freiburg, Germany, in 2007. The same year he joined the Berkeley Lab as a postdoctoral fellow. After a short stay at SRI International, where he studied atmospherically relevant processes, he returned to the Berkeley Lab to lead an effort for developing novel soft x-ray spectroscopies on nanoscale systems. He also investigates fundamental processes in EUV induced chemistry.

Frances A. Houle received her doctorate in chemistry at the California Institute of Technology. She has held appointments at the IBM Research Division and Invisage Technologies, and is now a Senior Scientist at Lawrence Berkeley National Laboratory. Her current research focuses on chemical processes in EUV photolithography and solar photochemistry for energy conversion. She has received numerous awards including an IBM Corporate Award and the AVS John A. Thornton Memorial Award and Lecture. She has published more than 170 scientific papers, and has 28 issued U.S. Patents. ORCID: 0000-0001-5571-2548